

# PHOBOS Beam Use Proposal for RHIC Runs IV-VIII

## The PHOBOS Collaboration

B.B.Back<sup>1</sup>, M.D.Baker<sup>2</sup>, M.Ballintijn<sup>4</sup>, D.S.Barton<sup>2</sup>, B.Becker<sup>2</sup>,  
R.R.Betts<sup>6</sup>, A.A.Bickley<sup>7</sup>, R.Bindel<sup>7</sup>, W.Busza<sup>4</sup>, A.Carroll<sup>2</sup>,  
M.P.Decowski<sup>4</sup>, E.García<sup>6</sup>, T.Gburek<sup>3</sup>, N.George<sup>2</sup>, K.Gulbrandsen<sup>4</sup>,  
S.Gushue<sup>2</sup>, C.Halliwell<sup>6</sup>, J.Hamblen<sup>8</sup>, A.S.Harrington<sup>8</sup>, C.Henderson<sup>4</sup>,  
D.J.Hofman<sup>6</sup>, R.S.Hollis<sup>6</sup>, R.Hołyński<sup>3</sup>, B.Holzman<sup>2</sup>, A.Iordanova<sup>6</sup>,  
E.Johnson<sup>8</sup>, J.L.Kane<sup>4</sup>, N.Khan<sup>8</sup>, P.Kulinich<sup>4</sup>, C.M.Kuo<sup>5</sup>, J.W.Lee<sup>4</sup>,  
W.T.Lin<sup>5</sup>, S.Manly<sup>8</sup>, A.C.Mignerey<sup>7</sup>, R.Nouicer<sup>2,6</sup>, A.Olszewski<sup>3</sup>, R.Pak<sup>2</sup>,  
I.C.Park<sup>8</sup>, H.Pernegger<sup>4</sup>, C.Reed<sup>4</sup>, C.Roland<sup>4</sup>, G.Roland<sup>4</sup>, J.Sagerer<sup>6</sup>,  
P.Sarin<sup>4</sup>, I.Sedykh<sup>2</sup>, W.Skulski<sup>8</sup>, C.E.Smith<sup>6</sup>, P.Steinberg<sup>2</sup>,  
G.S.F.Stephans<sup>4</sup>, A.Sukhanov<sup>2</sup>, M.B.Tonjes<sup>7</sup>, A.Trzupek<sup>3</sup>, C.Vale<sup>4</sup>,  
G.J.van Nieuwenhuizen<sup>4</sup>, R.Verdier<sup>4</sup>, G.I.Veres<sup>4</sup>, F.L.H.Wolfs<sup>8</sup>, B.Wosiek<sup>3</sup>,  
K.Woźniak<sup>3</sup>, B.Wysłouch<sup>4</sup>, J.Zhang<sup>4</sup>

<sup>1</sup> Argonne National Laboratory, Argonne, IL 60439-4843, USA

<sup>2</sup> Brookhaven National Laboratory, Upton, NY 11973-5000, USA

<sup>3</sup> Institute of Nuclear Physics, Kraków, Poland

<sup>4</sup> Massachusetts Institute of Technology, Cambridge, MA 02139-4307, USA

<sup>5</sup> National Central University, Chung-Li, Taiwan

<sup>6</sup> University of Illinois at Chicago, Chicago, IL 60607-7059, USA

<sup>7</sup> University of Maryland, College Park, MD 20742, USA

<sup>8</sup> University of Rochester, Rochester, NY 14627, USA

## 1 Overview

Over the past year, the RHIC collaborations have provided a wealth of new data. This included the first results from the d+Au run at RHIC [1], which showed the importance of studying collisions for different system sizes. At the same time, the CERN SPS experiments have analysed data from an energy scan with several intriguing results. The new insights provided by these data have further strengthened our view, as argued in previous beam use proposals, that a high statistics scan of the energy and system-size dependence of observables such as charged particle multiplicity, hadron yields at high  $p_T$ , elliptic flow and kaon  $p_T$  spectra, is the highest priority in the study of high energy heavy-ion collisions today.

We argue that such a survey, which could be performed over the next three RHIC running periods, will bring decisive progress in our understanding of the nature of nuclear matter under extreme conditions. For PHOBOS, these studies would then likely conclude the baseline program as outlined in the original proposal.

## 2 Status of PHOBOS

### 2.1 Run III PHOBOS Performance

The main goal of PHOBOS for the recent RHIC Run III was the detailed study of the centrality dependence of charged hadron multiplicities, spectra and particle ratios in d+Au collisions, as well as an increase of our data set on p+p collisions at  $\sqrt{s_{NN}} = 200$  GeV. In preparation for the run, a number of upgrades of the PHOBOS detector were implemented, commissioned and successfully operated. The upgrades included:

**DAQ upgrade** The DAQ was significantly upgraded in Run III. The raw data rate from the tunnel was increased to 240 MB/s. Lossless data compression was implemented, resulting in data volume reduction by a factor of 3.5. The VME connection between the Data Collector and Event Builder was replaced by a faster FPDP link (60 MB/s). As a result the data-taking rate was increased from 30 to 250 Hz.

**Forward Proton Calorimeter** Before and during the 2003 d+Au run, two proton calorimeters (PCAL) were installed in Phobos. These are designed to detect projectile protons which are at or near beam velocity (i.e. spectators). The detectors are comprised of  $10 \times 10 \times 117$  cm<sup>3</sup> lead scintillator modules. On the outgoing side for the Au projectile, a full size array was installed which is 8 modules in the bend plane direction and 10 modules high. On the outgoing side for the deuteron, the expected signal is essentially digital (either one or no proton), so only a smaller 2x2 array was installed. For the larger array, additional modules above and below the detector are used to trigger on cosmic rays for calibration purposes. Pedestals and gains were found to be very stable over the length of the run. Tests with different voltages showed no evidence for saturation even at values well above the nominal ones. The distribution of the signal in the Au side array was found to scale closely with the predicted number of spectators from a Glauber

model. Fine tuning of the gains and detailed comparisons to simulations are ongoing.

**New T0 Detectors** In anticipation of the lower charged-particle multiplicities expected in run III, compared to Au + Au, we increased the number of T0 detectors from 8 to 20. New support structures were designed such that these detectors can be installed at different positions along the beam-line, to optimize their efficiency for the type of collisions being studied. The timing signals from the T0 counters are aligned in time using time-equalizer modules, and the OR of the aligned timing signals is used to generate the time of the collision and an online vertex. The online vertex, which was reconstructed with a resolution of 3 - 4 cm, was used in making the PHOBOS trigger decision. The increase in the number of T0 detectors, coupled with the change in their positions, resulted in a significant increase in our efficiency to generate an online vertex, even in pp running.

**Spectrometer trigger** The goal of the Spectrometer Trigger was to enhance the yield of high-momentum particles in the PHOBOS Spectrometer and Time-Of-Flight acceptance, for d+Au and p+p collisions.

Two new scintillator-hodoscopes were installed and the existing PHOBOS TOF walls were incorporated into the triggering-system. Hit positions in these detectors, in combination with the event vertex, were used to select straight-line track trajectories corresponding to high-momentum particles. The online decision was made in under 15 ns using a programmable logic module. The Spectrometer Trigger efficiency was greater than 99% for particles with momentum above 2 GeV, while events with lower momentum particles were suppressed. As a result, the yield of TOF tracks per event at high- $p_T$  was enhanced by a factor of 15 relative to a minimum-bias trigger.

The total number of events collected during Run III was 200 million. The breakdown of events in different trigger types is shown in Table 1.

## 2.2 Recent PHOBOS results

### 2.2.1 Au+Au Analysis

Since our last report to the PAC, we have finalized and published or submitted results on the energy dependence of charged particle pseudo-rapidity distributions [2], the comparison of charged particle multiplicities in p+p,

Trigger Type	d+Au Events	p+p Events
MinBias	36M	40M
Vertex	38M	0.3M
SpecTrig	52M	10M
Peripheral	20M	0

Table 1: Summary of PHOBOS event totals for PR03, broken down by trigger type. ‘MinBias’ is the standard minimum-bias trigger; ‘Vertex’ events were required to have an online vertex within  $\pm 20$  cm of the nominal interaction point; ‘SpecTrig’ events satisfied the conditions for the high-momentum Spectrometer Trigger; and for d+Au collisions, ‘Peripheral’ events are defined by a low online multiplicity on the Au side.

A+A and  $e^+e^-$  [3] and the first measurement of the centrality dependence of charged particle spectra in 200 GeV Au+Au collisions [4], adding to the previous publications on charged hadron multiplicities [5, 6, 7, 8, 9], particle ratios [10, 11] and elliptic flow [12]. Analysis efforts on event anisotropies, identified particle spectra and particle correlations are ongoing.

### 2.2.2 d+Au Analysis

**d+Au Charged Hadron Spectra** As a first step in the analysis of d+Au data, we used the large coverage of our multiplicity detectors, as well as the additional information from the newly installed forward proton calorimeters, to study the determination of collision centrality in d+Au collisions. This was a critical element in our study of the centrality evolution of charged hadron  $p_T$  distributions in d+Au [1]. In this paper, we demonstrated that transverse momentum distributions in d+Au reach and may even exceed the expected binary collision scaling at high  $p_T$ . The observed centrality dependence is qualitatively different from that observed in Au+Au collisions at the same collision energy [4]. The results of this measurement are shown in Fig. 1 and 2. Fig. 1 shows the nuclear modification factor  $R_{dAu}$  as a function of  $p_T$  for each centrality bin. For comparison, the results from central Au+Au collisions at the same energy [4] are shown in the lower right panel of Fig. 1. The average number of collisions undergone by each participating nucleon in a central Au+Au collision is close to 6, similar to that of each nucleon from the deuteron in a central d+Au collision. For

central Au+Au collisions, the ratio of the spectra relative to  $p + \bar{p}$  rises rapidly up to  $p_T \approx 2$  GeV/c, but falls far short of collision scaling at larger  $p_T$ , in striking contrast to the behavior for d+Au collisions.

Perturbative QCD calculations [13] predicted an increase of 15% in the maximum value of  $R_{dAu}$  at  $p_T \approx 3.5$  GeV/c from peripheral to central events. In contrast, a decrease in  $R_{dAu}$  by 25–30% over the same centrality range was predicted in a parton saturation model [14]. The centrality evolution of  $R_{dAu}$  is shown in Fig. 2. Clearly, our data disfavor the prediction from the parton saturation model. This suggests that the observed suppression of high  $p_T$  hadrons in Au+Au collisions cannot be accounted for by initial state effects that should also be present in d+Au collisions.

### 3 Future PHOBOS Plans

#### 3.1 Future PHOBOS upgrades

**DAQ** The data-taking rate will be further increased to above 500 Hz, approaching the maximal rate provided by the front-end electronics of 700 Hz. To eliminate the bottleneck imposed by the existing RAID disk array, the disk array will be replaced by a dedicated data recorder (3.2 TB, 100 MB/s of sustained writing/reading).

**ToF** To improve the performance of the PHOBOS Time-of-Flight System, a new readout system based on a CERN designed high performance TDC will be installed in the RHIC tunnel close to the detector. The new system is anticipated to improve the time resolution to 100 ps, while eliminating issues related to cross-talk and propagation time drifts related to the present setup. This will allow proton identification up to a maximum  $p_T$  of 4.5 GeV/c.

**PCAL** As described above, the PCAL installation for the d+Au run required only a few modules on the outgoing side for the deuteron. In anticipation of Au+Au and possibly additional species in the upcoming run, the array on the 11 o'clock side is being expanded to a full-sized detector similar to that already in place on the 9 o'clock side.

#### 3.2 Status of RHIC physics

In the first three running periods, the four RHIC experiments have collected a wealth of high quality data over a wide range in collision energy and

centrality. PHOBOS has made significant contributions to the published and submitted physics output from the RHIC program [1-12]. For several observables, such as the strength of elliptic and radial flow or the systematics of particle spectra at large  $p_T$ , significant changes between the extremes in energy or system size are observed. The new data from the d+Au run show conclusively that the observed suppression at high  $p_T$  is a phenomenon that is unique to the large, high density system that is formed in Au+Au collisions. In combination, the results show that, in Au+Au collisions, an extremely high initial energy density is reached, as was suggested by the very first measurements three years ago [5].

### 3.2.1 Energy Scan

Several of the phenomena observed at RHIC, such as the high  $p_T$  suppression and the saturation of the hydrodynamic limit in elliptic flow, are not only unique to the large system created in Au+Au collisions, but also seem qualitatively different than has been observed in lower energy collisions at the CERN SPS. Of particular interest is the energy dependence of the suppression of high  $p_T$  particles. Existing measurements at RHIC and the SPS show that, over an order of magnitude in beam energy, the nuclear modification factor at intermediate  $p_T$  in central Au+Au collisions drops by more than a factor of 10, whereas the charged particle density only increases by a factor of 2. Yet, at the same time, many other observables show only a logarithmic energy dependence (e.g. mid-rapidity particle density) or remain approximately constant over an order of magnitude in collision energy (e.g. strangeness production, HBT radii). We have observed that just above the maximum SPS energy, the growth in the total charged particle multiplicity per participant pair seems to slow and show an energy dependence that is strikingly close to that of  $e^+e^-$  collisions in the same energy range [3], as can be seen in Fig. 3.

Recent results from the energy scan program at the CERN SPS, in comparison with the 130 and 200 GeV collider data from RHIC, have shown that several observables, like strange to non-strange particle ratios or average transverse momenta of strange particles, exhibit non-monotonic behaviour in their energy dependence. Striking examples are the systematics of kaon/pion ratios, which seem to show a exceedingly sharp maximum at  $\sqrt{s_{NN}} \approx 5$  GeV and the mean  $p_T$  of charged kaons, which rises with energy over the AGS energy range, shows a plateau at the SPS energy range and continues to rise again in the RHIC regime, reminiscent of the early

suggestions of Van Hove.

### 3.2.2 Species Scan

In addition to the energy dependence, the onset of the phenomena observed at the highest RHIC energies as a function of system-size needs to be studied in detail. Many of the most interesting new observables at RHIC have been shown to share common features in their centrality dependence, where a rapid change from p+p to peripheral Au+Au is followed by a relatively weak centrality dependence from peripheral to the most central Au+Au collisions. One example of this effect is illustrated by the hadron  $p_T$  distributions shown in Fig. 4, where a dramatic change in spectral shape occurs between p+p and the most peripheral bin in Au+Au, with approximately 60 participants. Another example is the total charged particle multiplicity, which is found to change rapidly from p+p to peripheral Au+Au collisions, but then remains constant [3].

Furthermore, results from lower energies suggest that for other observables such as e. g. strangeness production, neither  $N_{part}$  nor  $N_{coll}$  are the appropriate scaling variables [15]. The question of surface vs. volume contributions plays an important role in the interpretation of these results. A quantitative analysis of such phenomena depends on good experimental control of e.g. the number of participating nucleons.

The detailed interpretation of these effects, in particular for observables that need to be normalized by the number of participating nucleon pairs (e.g. the charged particle multiplicity), is severely hindered by the fact that a precise determination of  $N_{part}$  becomes increasingly difficult at large impact parameters, due to the uncertainty in the fraction of the total cross section to which the experiments are sensitive. For example, in the PHOBOS measurements of the charged particle multiplicity per participant pair, the uncertainty in the number of participants is the dominant contribution to the systematic uncertainty for peripheral events, exceeding 10% for bins with less than 50 participants and increasing rapidly with decreasing centrality.

A run with a lighter ion species such as Fe would provide the additional information needed to disentangle experimental and theoretical uncertainties in the understanding of the centrality dependence of the state produced in heavy-ion collisions.

### 3.2.3 Summary

**We argue that the largest conceptual advances in our understanding of the dynamical evolution of heavy-ion collisions and their connection to the QCD phase diagram will come from a comprehensive study of the energy dependence and system size dependence of the observables mentioned above.**

We realize that there is a high overhead price to be paid whenever energy or species are changed, and that therefore, in any one run, the number of different conditions under which RHIC is operated must be small. Taking all of the above into consideration, our main request is that a plan be developed to map out the complete RHIC landscape over the next three runs, using a variety of energies and colliding species. A detailed proposal for two initial runs with a different ion species and a lower collision energy is given below. Based on the results from these runs, we would finalize our choice of an additional energy and ion species for the following run, thus concluding the PHOBOS baseline program.

## 4 PHOBOS Physics Topics and Run Plan for Runs IV to VI

Below, we discuss the detailed implementation of the energy and species scan for the next three runs in the context of a strawman run plan. This plan would allow us to complete the baseline PHOBOS physics program in an optimal fashion. The assumed integrated luminosities, event rates and proposed running time for each of the different beam conditions can be found in Tables 2 and 3, assuming 37 and 27 weeks of RHIC running per year, respectively. The assumptions on the machine performance were based on the estimates provided in the document by Roser and Fischer [16]. We have used an overall combined uptime of experiment and machine of 25% and operation with  $\beta^* = 3$  m in the PHOBOS area. 50% of the events in the PHOBOS interaction region were assumed to fall into the usable vertex range of  $-20 \text{ cm} < z_{vtx} < +15 \text{ cm}$ , which requires operation of the 200 MHz storage cavities at full voltage. For the lower energy, the luminosity was assumed to scale with the square of the beam energy. Based on these assumptions, our event rate to tape will be DAQ-limited for minimum-bias p+p running and luminosity limited for all heavy ion running, as well as p+p running using the Spectrometer Trigger.



## 4.1 Physics Goals

Below we list the main physics goals for each of the requested run modes. For each mode, the topic with the largest required event statistics is listed first. The quoted range in the  $p_T$ -reach for each mode illustrates the uncertainty due to the range in integrated luminosities in Tables 2 and 3.

### **Au+Au at $\sqrt{s_{NN}} = 200$ GeV**

- $\phi$  spectrum and line shape at low  $p_T$  ( $< 200$  MeV/c) for central events.
- Identified particle spectra from low ( $< 50$  MeV/c) to high  $p_T$  (4.5 GeV/c for protons), also as a function of centrality and reaction plane.
- Charged hadron spectra at high  $p_T$  (6 – 8 GeV/c), also as a function of rapidity and reaction plane.
- Charged  $\pi$ -HBT as a function of centrality, rapidity and reaction plane.
- Elliptic flow vs  $\eta$  and  $p_T$ .
- Event-by-event fluctuations in multiplicity in different regions of  $\eta$ .
- Event-by-event fluctuations at low  $p_T$  near mid-rapidity.

### **Fe+Fe at $\sqrt{s_{NN}} = 200$ GeV**

- Charged hadron  $p_T$ -spectra out to  $p_T \approx 5-6$  GeV/c, also as a function of centrality and reaction plane.
- Identified particle spectra from low ( $< 50$  MeV/c) to high  $p_T$  (4.5 GeV/c for protons), also as a function of centrality and reaction plane.
- Particle ratios as a function of centrality and  $p_T$ .
- Charged  $\pi$ -HBT as a function of centrality and rapidity.
- Elliptic flow vs  $\eta$  and  $p_T$ .
- Pseudo-rapidity distributions in  $4\pi$  vs centrality.
- Event-by-event multiplicity fluctuations in different regions of  $\eta$ .
- Event-by-event fluctuations at low  $p_T$  near mid-rapidity.

**p+p at  $\sqrt{s_{NN}} = 200$  GeV**

- Charged hadron  $p_T$ -spectra out to  $p_T \approx 4 - 5$  GeV/c in the forward rapidity region ( $\eta \approx 1$ ) which is not covered by STAR/PHENIX.
- Identified particle spectra from low ( $< 50$  MeV/c) to high  $p_T$  ( $> 4$  GeV/c for protons).
- Event-by-event multiplicity fluctuations in different regions of  $\eta$ .

**Au+Au at  $\sqrt{s_{NN}} = 63$  GeV**

- Charged hadron  $p_T$ -spectra out to  $p_T \approx 4 - 4.5$  GeV/c as a function of centrality.
- Identified particle spectra from low ( $< 50$  MeV/c) to high  $p_T$  (3.5 GeV/c for protons), as a function of centrality and reaction plane.
- Particle ratios as a function of centrality and  $p_T$ .
- Charged  $\pi$ -HBT as a function of centrality and rapidity.
- Elliptic flow vs  $\eta$  and  $p_T$ .
- Pseudo-rapidity distributions in  $4\pi$  vs centrality.
- Event-by-event multiplicity fluctuations in different regions of  $\eta$ .

**p+p at  $\sqrt{s_{NN}} = 500$  GeV** A short run at the highest energy would allow us to study p+p collisions with an effective center-of-mass energy closer to that in Au+Au at 200 GeV, after taking the leading baryon effect into account. This will allow us to further test the observed universality in hadron production [3].

- Charged hadron  $p_T$  distributions.
- Pseudo-rapidity distributions in  $4\pi$ .
- Particle ratios as a function of  $p_T$ .

**Further energy and/or species scan** We expect to run at one further energy and one further species after the initial scan. The details of these requests will be based on the analysis of the Au+Au run at  $\sqrt{s_{NN}} = 63$  GeV and the Fe+Fe run at  $\sqrt{s_{NN}} = 200$  GeV.

**Additional PHOBOS running** With the run plan described above, we expect to finish the PHOBOS baseline program with the data from runs IV to VI. Further running would only be requested if the PHOBOS detector was shown to be particularly well suited to answer concrete questions or resolve puzzles posed by the data from the energy or species scans.

#### 4.1.1 Proposed running schedule

In Tables 2 and 3 we show possible run plans for 37 weeks and 27 weeks of yearly RHIC running, respectively. The tables show the expected duration, integrated luminosity and good events to tape for each proposed running mode. We believe that it is essential to schedule the 200 GeV Fe+Fe run and the 63 GeV Au+Au run as early in the upcoming program as possible, enabling us to select the additional energies and species in the subsequent run based on the detailed analysis of the initial scan.

Run Mode	Delivered $\int Ldt$	Events on Tape	Running Time
Run IV			
Au+Au 200 GeV	100 - 260 $(\mu b)^{-1}$	300 - 640 M	18 weeks
Fe+Fe 200 GeV	90 - 210 $(\mu b)^{-1}$	90 - 190 M	6 weeks
Run V			
p+p 200 GeV	1.8 - 3 $(pb)^{-1}$	1400 M	12 weeks
Au+Au 63 GeV	4.8 - 12 $(\mu b)^{-1}$	18 - 45 M	12 weeks
Run VI			
p+p 500 GeV	1.4 - 1.8 $(pb)^{-1}$	480 M	4 weeks
Further Energy/Species			

Table 2: Proposed running schedule for 37 weeks of RHIC running/year

Run Mode	Delivered $\int Ldt$	Events on Tape	Running Time
Run IV			
Au+Au 200 GeV	33 - 90 $(\mu b)^{-1}$	110 - 240 M	10 weeks
Fe+Fe 200 GeV	42 - 110 $(\mu b)^{-1}$	50 - 110 M	4 weeks
Run V			
p+p 200 GeV	1.0 - 1.4 $(pb)^{-1}$	840 M	7 weeks
Au+Au 63 GeV	2.3 - 4.9 $(\mu b)^{-1}$	6 - 16 M	7 weeks
Run VI			
p+p 500 GeV	1.4 - 1.8 $(pb)^{-1}$	480 M	4 weeks
Further Energy/Species			

Table 3: Proposed running schedule for 27 weeks of RHIC running/year

## References

- [1] Centrality Dependence of the Charged Hadron Transverse Momentum Spectra in d+Au Collisions at  $\sqrt{s_{NN}} = 200$  GeV. B. B. Back *et al.*, Phys. Rev. Lett. **91** 072302 (2003).
- [2] Significance of the Fragmentation Region in Ultrarelativistic Heavy Ion Collisions  
B. B. Back *et al.*, Phys. Rev. Lett. **91**, 052303 (2003).
- [3] Comparison of the Total Charged-Particle Multiplicity in High-Energy Heavy Ion Collisions with  $e^+e^-$  and  $pp/\bar{p}p$  Data  
B. B. Back *et al.*, arXiv:nucl-ex/0301017, submitted to Phys. Rev. Lett.
- [4] Charged Hadron Transverse Momentum Distributions in Au+Au Collisions at  $\sqrt{s_{NN}} = 200$  GeV  
B. B. Back *et al.*, arXiv:nucl-ex/0302015, submitted to Phys. Lett. **B**.
- [5] Charged Particle Multiplicity Near Mid-rapidity in Central Au+Au Collisions at  $\sqrt{s_{NN}} = 56$  and 130 GeV,  
B. B. Back et al. Phys. Rev. Lett. **85**, 3100 (2000)
- [6] Charged-particle Pseudorapidity Density Distributions from Au+Au Collisions at  $\sqrt{s_{NN}} = 130$  GeV,  
B. B. Back et al. Phys. Rev. Lett. **87**, 102303 (2001)

- [7] Centrality Dependence of Charged Particle Multiplicity at Midrapidity in Au+Au Collisions at  $\sqrt{s_{NN}} = 130$  GeV,  
B. B. Back et al. Phys. Rev. **C65**, 31901R (2002)
- [8] Energy Dependence of Particle Multiplicities Near Mid-rapidity in Central Au+Au Collisions  
B. B. Back et al. Phys. Rev. Lett. **88**, 22302 (2002)
- [9] Centrality Dependence of the Charged Particle Multiplicity near Mid-rapidity in Au+Au Collisions at  $\sqrt{s_{NN}} = 130$  and 200 GeV  
B. B. Back et al. Phys. Rev. **C65**, 061901R (2002)
- [10] Ratios of Charged Particles to Antiparticles Near Mid-rapidity in Au+Au Collisions at  $\sqrt{s_{NN}} = 130$  GeV,  
B. B. Back et al. Phys. Rev. Lett. **87**, 102301 (2001)
- [11] Ratios of Charged Antiparticles to Particles Near Mid-rapidity in Au+Au Collisions at  $\sqrt{s_{NN}} = 200$  GeV  
B. B. Back *et al.*, Phys. Rev. **C67**, 021901R (2003).
- [12] Pseudorapidity and Centrality Dependence of the Collective Flow of Charged Particles in Au+Au Collisions at  $\sqrt{s_{NN}} = 130$  GeV  
B. B. Back *et al.*, Phys. Rev. Lett. **89**, 222301 (2002)
- [13] I. Vitev, arXiv:nucl-th/0302002.
- [14] D. Kharzeev, E. Levin, L. McLerran, BNL preprint BNL-NT-02/22, arXiv:hep-ph/0210332.
- [15] I. Kraus *et al.*, NA49 Collaboration, Proceedings of SQM 2003, Atlantic Beach, USA; J. Phys. G in press, arXiv:nucl-ex/0306022.
- [16] T. Roser and W. Fischer, RHIC Collider Projections (FY2004-FY2008), BNL, August 8, 2003.

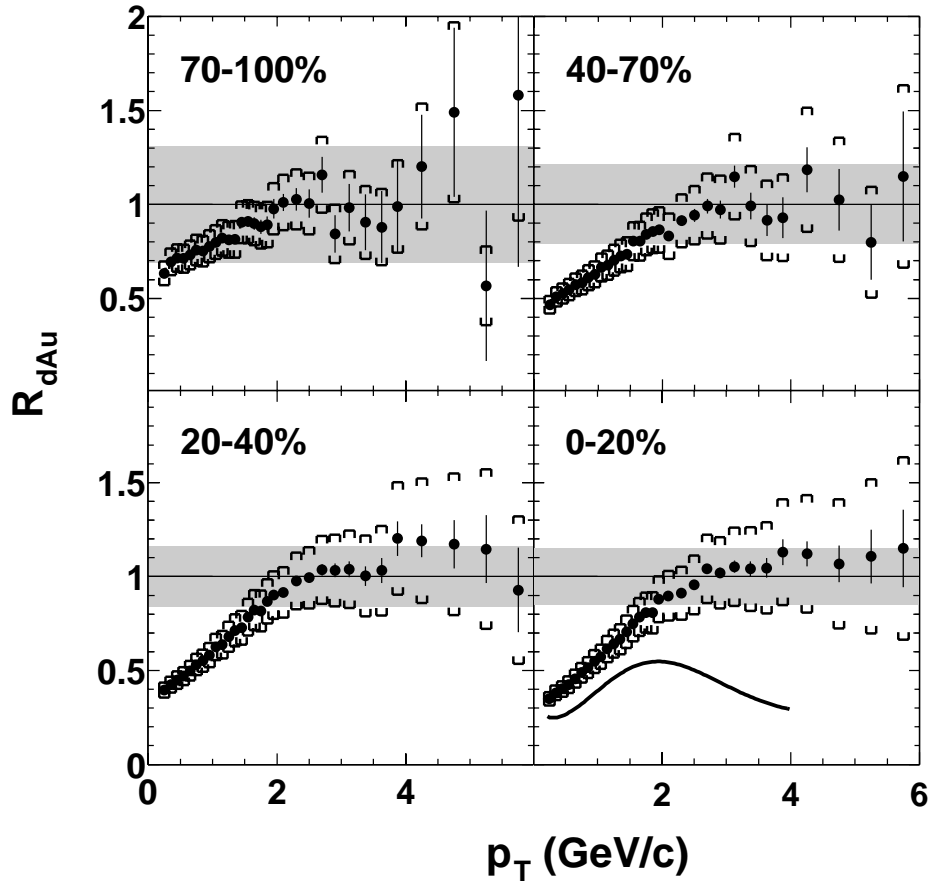


Figure 1: Nuclear modification factor  $R_{dAu}$  as a function of  $p_T$  measured in d+Au collisions at 200 GeV for four bins of centrality. For the most central bin, the spectral shape for central Au+Au data relative to  $p + \bar{p}$  is shown for comparison. The shaded area shows the uncertainty in  $R_{dAu}$  due to the systematic uncertainty in  $\langle N_{coll} \rangle$  and the UA1 scale error (90% C.L.). The brackets show the systematic uncertainty of the d+Au spectra measurement (90% C.L.).

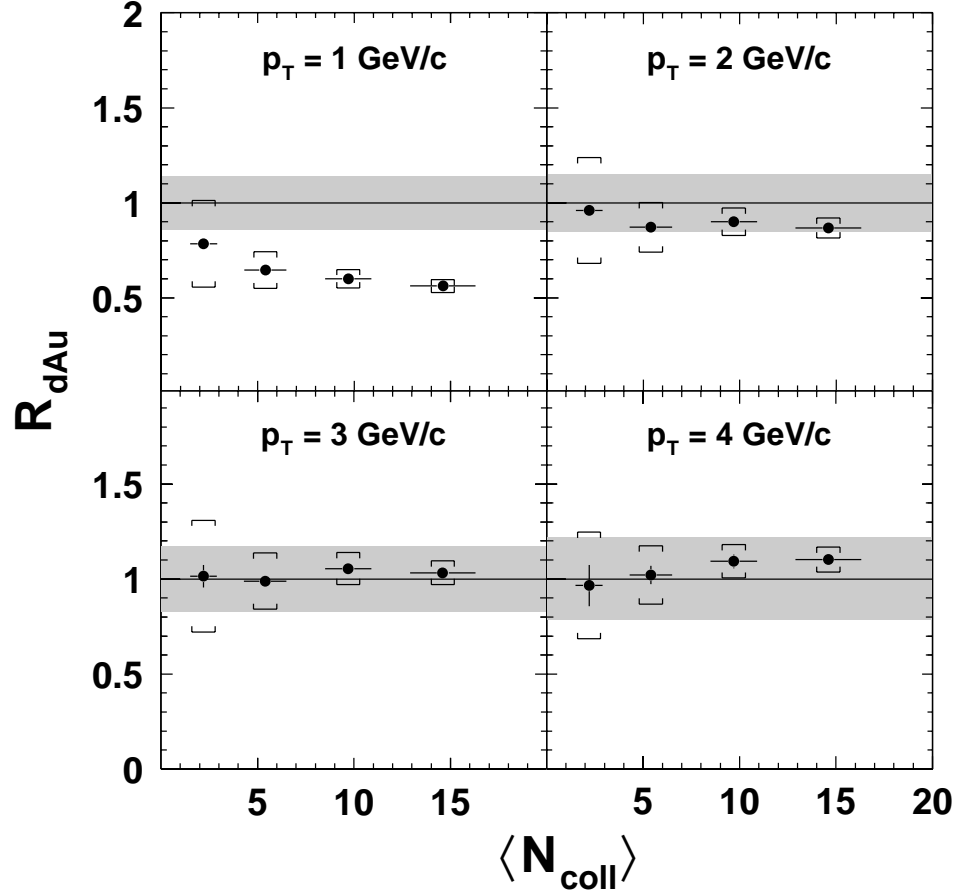


Figure 2: Nuclear modification factor  $R_{dAu}$  as a function of centrality in four bins of transverse momentum for d+Au collisions at 200 GeV. The brackets indicate the point-to-point systematic error, dominated by the uncertainty in the number of collisions for each centrality bin. The grey band shows the overall scale uncertainty at each  $p_T$ . Systematic errors are at 90% C.L.

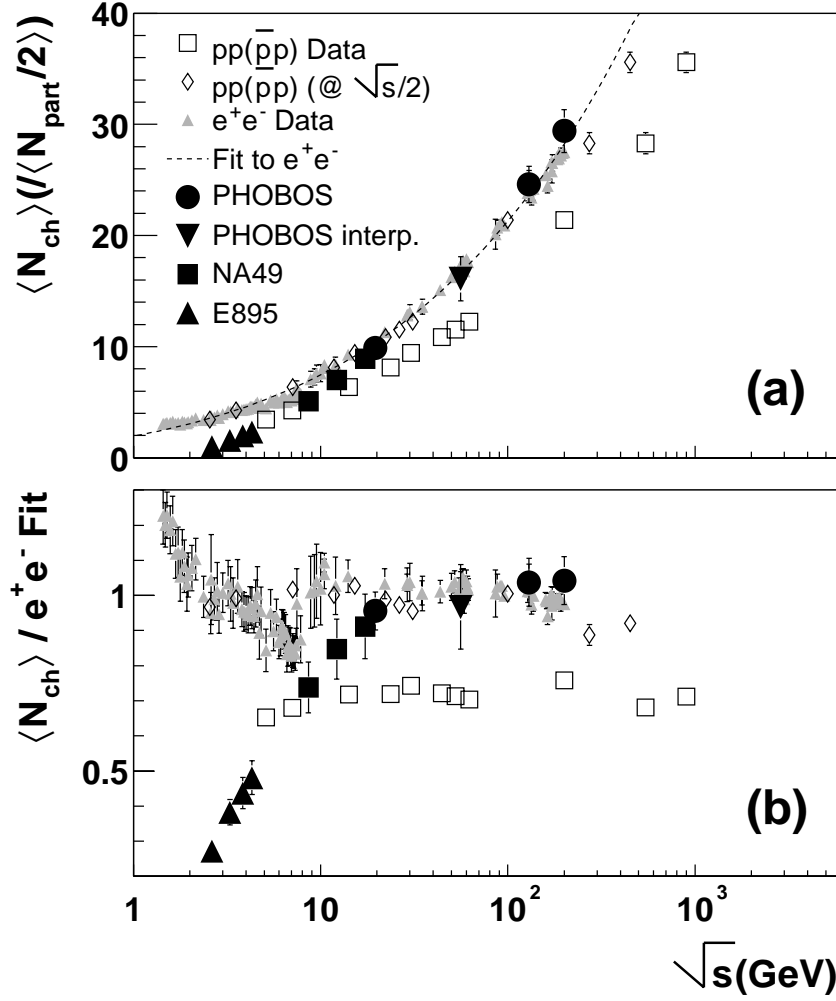


Figure 3: Comparison of the total charged multiplicity  $\langle N_{ch} \rangle$  for  $pp$ ,  $e^+e^-$  and central Au+Au events as a function of  $\sqrt{s}$ . The Au+Au data are normalized by  $N_{part}/2$ . In the lower plot, all data were divided by a fit to the  $e^+e^-$  data.



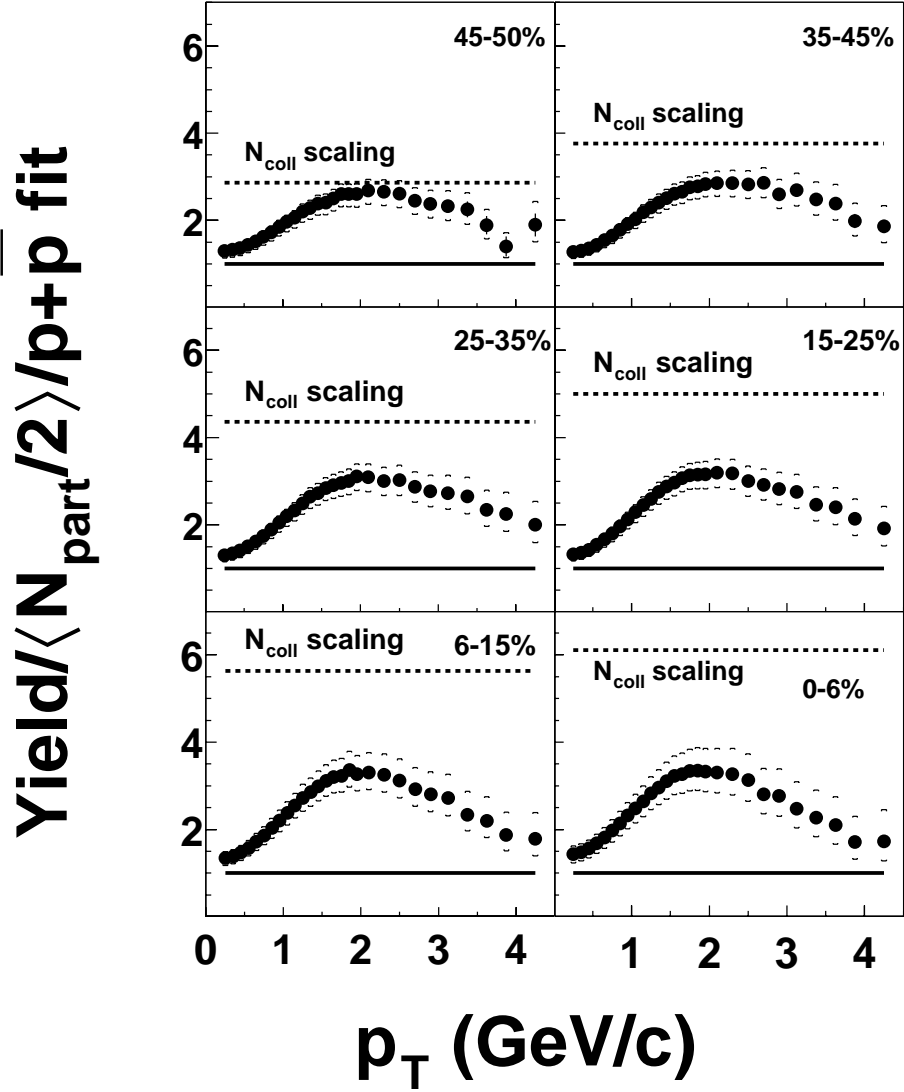


Figure 4: Ratio of the charged hadron  $p_T$  spectra for six centrality bins in Au+Au at 200 GeV collisions to a fit of proton-antiproton data scaled by  $\langle N_{part}/2 \rangle$ . The centrality bins range from  $\langle N_{part} \rangle = 65 \pm 4$  (upper left plot) to  $\langle N_{part} \rangle = 344 \pm 11$  (lower right plot). The dashed (solid) line shows the expectation of  $N_{coll}$  ( $N_{part}$ ) scaling relative to  $p + \bar{p}$  collisions. The brackets show the systematic uncertainty of the Au+Au data.